Area precipitation probabilities derived from point forecasts for operational weather and warning service applications

Reinhold Hess[a]*, Bjoern Kriesche[b], Peter Schaumann[b], Bernhard K. Reichert[a], Volker Schmidt[b]

[a]*Deutscher Wetterdienst, Frankfurter Straße 135, 63067 Offenbach, Germany*

[b]*Ulm University, Institute of Stochastics, Helmholtzstraße 18, 89069 Ulm, Germany*

*Correspondence to: Deutscher Wetterdienst, Frankfurter Straße 135, 63067 Offenbach, Germany. E-mail: reinhold.hess@dwd.de

Probabilistic precipitation forecasts of numerical models are often calibrated using synoptic observations. The resulting probabilities of precipitation refer to the observation system and thus provide the likelihood that precipitation occurs exactly at the spot of the ombrometer. When probabilistic forecasts for larger areas, such as rural districts or catchment areas of rivers, are required, it is not possible to interpolate the point probabilities. Instead area probabilities e.g. increase with the size of the area. In this paper we describe a general method to derive area probabilities from point forecasts based on models and methods of stochastic geometry. The method can be applied on arbitrary areas and can be used for operational applications, since it runs fully automatically without human interaction. The basic idea is to model precipitation patterns by circular precipitation cells using a germ–grain model driven by a spatial Poisson point process in a way that the point forecasts are fitted. Area probabilities can then be estimated statistically as relative frequencies based on repeated Monte Carlo simulations. As the area probabilities significantly depend on the sizes of the modeled precipitation cells, suitable cell radii are estimated based on the spatial correlation structure of given point probabilities. Verification with independent radar precipitation and comparison with area probabilities derived from the raw ensemble system COSMO-DE-EPS of DWD is provided and reveals essential advantages of the stochastic model in terms of bias and Brier skill score.

Key Words: Probabilistic weather prediction, weather warning, area probability, stochastic model, precipitation

Received . . .

1. Introduction

1.1. Automated warning guidances

One of the main statutory tasks of the Deutscher Wetterdienst (DWD) and of various other national weather centres worldwide is the issuance of official warnings of weather occurrences that could become a danger for public safety and order. Some of the key customers range from civil protection, federal and regional authorities, provincial administrations of road construction, winter services, municipalities, business companies and media, up to private customers and the general public. This wide range of customers requires a variety of warning products tailored to individual customer's needs.

In recent years, DWD has operationally introduced the Warning Decision Support System AutoWARN, see Reichert (2010, 2017) and Reichert *et al.* (2015). One aim is to help forecasters deal with increasing amounts of numerical weather prediction (NWP) and ensemble forecasts, as well as observational and nowcasting data by providing integrated automated warning proposals. These warning proposals can be accepted or manually modified by forecasters who bear final responsibility for official warnings of DWD. The result is a final warning status used to automatically produce the full range of individual textual and graphical warning products for customers. These automatic products include Internet and mobile app visualisations for about 11,000 German municipalities with a high update frequency as well as more coarse warning products in space and time for individual client needs.

Currently, these warning products are mainly issued in a deterministic way, e.g. a heavy rain warning may or may not exist for a specific municipality. However, customers more and more demand probability–based warning products, answering questions on the likelihood of occurrence e.g. for a heavy rain warning event. Using individual cost–loss ratios customers may use calibrated probability information in order to take appropriate actions on specific probability threshold levels and e.g. minimise costs for their specific case.

A prerequisite for exploiting the full potential of probability–based warning information is to provide calibrated probability information on desired areas of interest, e.g. on dedicated warning regions for customers. Area probabilities thereby take into account that the exact location of a warning event is usually unknown.

Therefore, upscaling in space according to forecast predictability is required.

Approaches exist that derive area probabilities from ensembles of precipitation fields. Assuming fractal characteristics of precipitation deterministic NWP models can be used to downscale precipitation and to produce ensembles of precipitation fields on a continuum of scales, like STEPS, see Bowler *et al.* (2006). Ensembles of precipitation fields can also be obtained from ensemble prediction systems like COSMO-DE-EPS, where estimations of precipitation probabilities can be derived for aggregations of grid points as relative frequencies of occurrences, see Sec. 2.1. In order to derive calibrated area probabilities calibrated sets of ensemble members are required. Approaches as copula coupling or Shaake shuffle, see e.g. Schefzik *et al.* (2013) or Hamill *et al.* (2017), optimize mean and spread of a raw NWP ensemble and construct an optimized ensemble having these optimized statistical properties. In order to allow the forecaster to define the precipitation areas they are interested in ad hoc, the full set of ensemble members needs to be held available for computation upon request.

Against this background, the present paper describes a new way to derive warn–relevant precipitation probabilities for arbitrary areas based on point forecasts. The approach is applied to the output of an Ensemble Model Output Statistics (EnsembleMOS)–based system, see Hess *et al.* (2015), operationally used within the AutoWARN warning process chain at DWD as described above. The ensemble information is extracted as early as possible in order to reduce computational and memory costs and to provide a fast and flexible system. As the forecaster in principle may have the possibility to manually modify the point probabilities of the EnsembleMOS output, the method proposed in this paper opens up a new way of providing customer specific, area–based automatic precipitation probability products derived from statistically postprocessed and manually controlled NWP ensemble forecasts.

1.2. Point and area probabilities

We define an area probability, strictly speaking, as the probability that a certain event occurs at least once anywhere in the area of interest. This notion of an area probability is qualitatively different from a point probability that expresses the chance that the occurrence takes place exactly at a fixed point. An area probability is always larger than any point probability within that area and grows with the size of the area. Here, the spatial scale of the meteorological events plays an essential role. Large–scale events with a high degree of spatial correlation can result in area probabilities, which are only a little higher than point probabilities. However the smaller the scale of the event, the less the point probabilities are correlated and the faster the area probability grows with the size of the area.

Probabilistic forecasts of numerical models can be calibrated using relative frequencies of observed occurrences of meteorological events such as wind gusts or precipitation. The meteorological observations from rain gauges and anemometers provide in–situ measurements, which are representative for small areas (e.g. several centimeters in diameter for rain gauges) that can be mathematically considered as points. Synoptic observation sites usually are located at places, which are most representative for their surroundings. Nevertheless, there always exist differences between the point measurement and values at other locations kilometers apart, or between the point measurement and area averages as they are provided by numerical models with typical resolutions of several kilometers, e.g. 2.8 km for the regional model COSMO-DE* of DWD, see Baldauf *et al.* (2011). In meteorology these differences are known and addressed as errors of representativity.

When it comes to probabilistic forecasting, event probabilities are still related to points as far as they are calibrated using in–situ measurements as described in Sec. 2.2. Clearly, the point probabilities provide information about their surroundings due to statistical spatial correlations of precipitation events. Known analytical formulas to directly derive area probabilities from point probabilities are not operationally applicable, however. Approaches of Epstein (1966) and Krzysztofowicz (1998) assume circular precipitation cells, uniformly distributed cell centres and circular forecast areas to find theoretical scaling equations. The diameters of precipitation cells are found to be crucial for their results, but they need to be quantified by the forecaster for the current meteorological situation or estimated from climatic data.

As an alternative to the application of direct computation formulas we suggest to determine area probabilities using spatial stochastic models for precipitation, see e.g. Onof *et al.* (2000), Wheater *et al.* (2000) or Wheater *et al.* (2005). An algorithmic method to derive area probabilities from point probabilities based on a generally applicable stochastic model for precipitation cells is presented in Kriesche *et al.* (2015). This method estimates the radii of the precipitation cells depending on the spatial correlations of the provided point probabilities for the current meteorological situation. Moreover, the prescribed methods of stochastic geometry provide mathematical background for relating area and point probabilities in general and applying it in other contexts, such as verification of model data with in–situ observations or changing the grid resolution of probabilities from numerical ensemble systems, without the need for a complete set of ensemble members. Kriesche *et al.* (2015) focuses on the mathematical and technical details of the method, whereas in the present paper we address aspects of its applicability and concentrate on forecast results and verification.

1.3. Outline

The outline of the paper is as follows: after motivation and general description of the research given in Sec. 1 the COSMO-DE-EPS (Ensemble Prediction System of COSMO-DE) and its statistical postprocessing EnsembleMOS are introduced in Sec. 2 in order to prescribe the estimation of calibrated point probabilities. Section 3 provides an overview of the stochastic model for precipitation that allows for the estimation of area probabilities based on point probabilities. This model is validated in Sec. 4 by means of independent radar data (Sec. 4.1) and by sensitivity studies for the precipitation cell radii (Sec. 4.2). Moreover, Sec. 4.3 presents a comparison of estimated area probabilities with uncalibrated and upscaled relative frequencies of the ensemble system COSMO-DE-EPS. Finally, Sec. 5 provides conclusions and an outlook.

2. The EnsembleMOS for COSMO-DE-EPS

For ensemble prediction systems, ensembles of forecasts are computed that differ in initial and boundary conditions as well as in physical parameterisation within the scale of uncertainty. The resulting distribution of forecasts and, in particular, the forecast variances provide essential information on forecast reliability and accuracy. Ideally, the standard deviation between ensemble members (ensemble spread) should statistically fit the error of the ensemble mean against synoptic observations (skill).

* The COSMO–model is the forecast model of the COnsortium for Small–scale MOdeling at which DWD is member. COSMO-DE is the specific version for Germany of DWD.

However, especially near the surface ensemble forecasts are often underdispersed, see e.g. Gebhardt *et al.* (2011) .

In order to derive probabilistic forecasts that correspond statistically to experienced event frequencies, postprocessing for statistical calibration is often applied. At DWD the COSMO-DE-EPS is calibrated by EnsembleMOS, which is a model output statistics (MOS) system specialised for the statistical optimisation of ensembles and for the calibration of probabilistic forecasts. A brief overview of the COSMO-DE-EPS and EnsembleMOS is given in the following. Further information is available in the provided references.

2.1. The ensemble system COSMO-DE-EPS and upscaled precipitation probabilities

The ensemble system COSMO-DE-EPS of DWD is based on the numerical model COSMO-DE. It currently consists of 20 ensemble members and provides weather forecasts for Germany with a resolution of 2.8 km. The forecasts are computed and issued every three hours with a forecast range up to 27 hours ahead. Detailed descriptions of COSMO-DE and its ensemble system COSMO-DE-EPS are provided in Baldauf *et al.* (2011) and Gebhardt *et al.* (2011), respectively. For each of the ensemble members initial and boundary conditions as well as physical parameterisations of COSMO-DE are varied according to assumed uncertainty. The obtained forecasts provide information on the distribution of possible weather regimes to be expected. For example, the standard deviation of the ensemble is an estimate of the accuracy of the ensemble mean compared to observations, see e.g. Wilks (2011) .

Probabilistic forecasts can be estimated as the relative frequency of event occurrence in the ensemble members. This frequency can be evaluated grid point by grid point resulting in probabilities corresponding to the original resolution of COSMO-DE with areas of $2.8^2\,\mathrm{km}^2$. For precipitation also upscaled probabilities are derived in this way, which refer to larger areas of 10×10 grid points ($28^2\,\mathrm{km}^2$). The meteorological event that precipitation rate exceeds a certain threshold in an area is considered to occur for a member if the threshold is exceeded at any one of the 100 points of such an area. The relative number of ensemble members that show the event provides an estimate of the area probability. Hereby it is not required that the events take place at the same grid points in the area. The resulting upscaled probabilities correspond to our definition of area probabilities that implies that an event occurs at least once anywhere (spatially continuous) in that area.

These raw ensemble–derived probabilities are not calibrated using synoptic observations. Verifications with independent radar data and comparisons to area probabilities based on calibrated point probabilities as modeled in Sec. 3.3 are provided in Sec. 4.3 .

2.2. EnsembleMOS and calibrated point probabilities

The EnsembleMOS of DWD is a MOS system fitted for statistical optimisation and calibration of ensemble forecasts such as COSMO-DE-EPS or IFS-EPS. The latter is the ensemble prediction system of the Integrated Forecasting System (IFS) of the European Centre for Medium–Range Weather Forecasting (ECMWF). Compared to MOS systems for deterministic forecasts, the EnsembleMOS is set up to use ensemble products such as ensemble mean, spread and quantiles as predictors instead of deterministic forecasts. The EnsembleMOS is based on a MOS system originally set up for postprocessing deterministic forecasts of the former numerical model GME of DWD and the IFS of ECMWF, see Knüpffer (1996) . For an introduction to MOS in general we refer to Wilks (2011) .

For statistical optimisation, interpretation and calibration of the COSMO-DE-EPS, historical time series of more than 300 synoptic stations within Germany and its surrounding are used. The time series currently range from 2011 up to 2015 and are extended regularly. In order to provide reasonably large data sets for extreme and rare weather events, the synoptical stations are grouped together in nine climatic zones (e.g. coastal strip, north German plain, various height zones in southern Germany, high mountains areas, etc.). Stepwise regression is performed for all stations in these zones together.

More than 150 forecasting elements are computed with lead times up to 21 hours ahead in hourly intervals, see also Sec. 2.3 . These forecasting elements comprise of series of event probabilities for various thresholds and reference periods, such as e.g. the probability that the rain amount exceeds 15 mm in one hour or that wind gusts exceed 14 m/s during an interval of three hours.

For each predictand (i.e. forecast element) the most relevant predictors out of a set of about 300 model elements and observations are selected as long as they are statistically significant using stepwise regression. For continuous variables, such as precipitation amount or wind speed, linear regression is applied. Logistic regression is used for probabilistic predictands such as threshold exceedances. Most predictors are derived from the underlying numerical model, but the latest available observations are also provided as predictors and are frequently selected for short range forecasts according to meteorological persistence. EnsembleMOS uses probabilistic products of the ensemble as model predictors, such as ensemble mean and standard deviation. Systems that optimise each ensemble member individually are prone to underdispersed forecasts and too small error estimates as they tend towards climatology for longer forecast ranges. This problem is avoided by using ensemble products as predictors within EnsembleMOS.

The stepwise regression results in a selection of predictors and coefficients for each predictand and climatic zone that form an equation for the specific predictand. For operational forecasting this equation of predictors and coefficients can be evaluated with current values of observations and the numerical model in order to provide optimised forecasts. The equation may be applied at the original observation sites or at any other place within the climatic zone. If necessary, the observations need to be interpolated to the specified location. The numerical model however is always evaluated for the exact location, i.e. the next grid point of the numerical model.

2.3. Input point probabilities for the stochastic model

For the present study point probabilities for precipitation exceeding 0.1 mm within one hour have been generated on a regular grid of 20 km resolution covering Germany. The point forecasts are computed by postprocessing the COSMO-DE-EPS according to the climatic zones the grid points belong to, as described in Sec. 2.2 .

The period from 1 May until 31 July 2016 has been selected that includes a number of heavy precipitation events. The COSMO-DE-EPS runs every three hours and its postprocessing that generates the calibrated point precipitation probabilities is issued two hours after the start of the COSMO-DE-EPS when its computation has normally finished.

Postprocessed forecasts are provided for hourly lead times up to 21 hours ahead. However, most results presented in this paper are based on forecasts up to 3 hours ahead in order to use point forecasts with short lead times and best accuracy as input for the stochastic model of the area probabilities. Deteriorations of the stochastic model and the area probabilities become most apparent

in this way. Since COSMO-DE-EPS and related point forecasts are updated every three hours, the use of 1 to 3 hourly optimized forecasts allows for a continuous verification in time without overlaps of forecast intervals.

3. Area precipitation probabilities

The proposed method for the derivation of area probabilities is based on a spatially continuous stochastic model for precipitation cells. We give a brief overview of this method in the following. A more detailed description can be found in Kriesche *et al.* (2015, 2017a) , where the latter paper applies to the modeling of thunderstorm cells.

The basic idea is to model precipitation patterns based on random circular precipitation cells, see Sec. 3.1. Accordingly, it is assumed that there is precipitation at any given point if and only if this point is covered by at least one precipitation cell. The parameters of the stochastic model of precipitation cells are estimated in such a way that point probabilities derived from the model match those probabilities from the available data and their correlation structure, see Sec. 3.2 . Based on the fitted model, the area probability for an arbitrary area can then be derived as the probability that this area is at least partially covered by one of the random precipitation cells. This is more formally stated in Sec. 3.3 . The sizes of the precipitation cells influence the spatial correlation structure of modeled precipitation patterns and are essential for the spatial expansion from point to area probabilities. The radii of the circular precipitation cells, which are parameters of the stochastic model with a meteorological interpretation, are estimated spatially constant but fitted for the current meteorological situation, in order to address different spatial correlations of convective events and large scale precipitation scenarios. Statistics of estimated precipitation cell radii are provided in Sec. 4.2 .

3.1. Stochastic model for precipitation cells

We give a brief, simplified overview of the underlying stochastic model for precipitation cells. Consider a fixed one–hour forecast period with an arbitrary lead time and let $s_1, \ldots, s_n \in W$ denote the $n = 1,786$ locations of grid points of a regular 20 km $\times$ 20 km grid in a rectangular observation window W comprising the domain of Germany. By $p_{s_1}, \ldots, p_{s_n}$ we denote the point probabilities at $s_1, \ldots, s_n$ that are available in the data described in Sec. 2.3. Centres of precipitation cells are modeled using a spatial Poisson process $\{X_i,\, i = 1, \ldots, Z\}$ in W with intensity function $\{\lambda_t, t \in W\}$, see Chiu *et al.* (2013), where Z is a random variable that describes the number of cell centres in W. For each location t the intensity λ_t can be interpreted, roughly speaking, as the expected number of cell centres in a unit area around t. To simplify the computations we suppose the intensity function to be piecewise constant, i.e.

$$\lambda_t = a_i \quad \text{for } t \text{ in } V(s_i),\ i = 1, \ldots, n \quad , \tag{1}$$

where $V(s_i)$ denotes the Voronoi cell[†] of grid point s_i in W and $a_1, \ldots, a_n$ are some non–negative intensities of precipitation cell occurrence. In particular, this allows for a spatially inhomogeneous distribution of precipitation cells, which is crucial for applications on a non–local scale. Each cell centre is attached with a radius r and the resulting discs $\{b(X_i, r),\, i = 1, \ldots, Z\}$ represent single precipitation cells. The union set

$$M = \bigcup_{i=1}^{Z} b(X_i, r) \tag{2}$$

is then used as a model for the spatial precipitation pattern in the considered forecast period. Area probabilities will be modeled as coverage probabilities of M, see Sec. 3.3.

3.2. Estimation of model parameters

In order to estimate area probabilities, the model M for the union set of precipitation cells has to be simulated repeatedly. For that purpose we first need to compute the parameters $a_1, \ldots, a_n$ and r based on the given point probabilities $p_{s_1}, \ldots, p_{s_n}$.

3.2.1. Estimation of intensity parameters

The intensity parameters $a_1, \ldots, a_n$ implicitly depend on the cell radius r . Thus, we assume temporarily that the optimal radius r of precipitation cells is known. A statistical approach to the computation of r is described in Sec. 3.2.2 . The basic modeling assumption is that there is precipitation at any given point t in W if and only if t is covered by the union set M, i.e. if $t \in M$. Accordingly, there is precipitation at grid point s_i if the disc $b(s_i, r)$ contains at least one random precipitation cell centre. Note that the random number of points of $\{X_i,\, i = 1, \ldots, Z\}$ falling into $b(s_i, r)$ has a Poisson distribution with mean value

$$n(s_i, r) = \sum_{j=1}^{n} a_j \, |b(s_i, r) \cap V(s_j)| \quad , \tag{3}$$

where $|S|$ denotes the area (i.e. the two–dimensional Lebesgue measure) for a subset $S \subset W$.

Therefore, the probability of precipitation at s_i is

$$p_{s_i} = P(s_i \in M) = 1 - e^{-\sum_{j=1}^{n} a_j \, |b(s_i, r) \cap V(s_j)|} \quad , \tag{4}$$

which is equivalent to

$$\ln\left(\frac{1}{1 - p_{s_i}}\right) = \sum_{j=1}^{n} a_j \, |b(s_i, r) \cap V(s_j)| \tag{5}$$

for $i = 1, \ldots, n$. This results in a system of n linear equations for the n unknowns $a_1, \ldots, a_n$. Due to the constraint that intensity functions cannot be negative, i.e. $a_j \geq 0$ for $j = 1, \ldots, n$ this system of equations can only be solved approximately using an optimisation algorithm. Verifications for actual cases however show sufficiently precise solutions, see Kriesche *et al.* (2015).

3.2.2. Estimation of cell radius

The cell radius r reflects the spatial precipitation range and is estimated globally constant for the forecast region. Larger precipitation cells cover wider areas, thus r is expected to be closely related to the spatial correlation structure of the point probabilities $p_{s_1}, \ldots, p_{s_n}$. For the quantification of spatial dependencies we suppose that $p_{s_1}, \ldots, p_{s_n}$ are realisations of some random field $\{P_t, t \in W\}$ at $s_1, \ldots, s_n$ and consider the semivariogram $\gamma : [0, \infty) \to [0, \infty)$ of $\{P_t, t \in W\}$ defined as

$$\gamma(||t_1 - t_2||) = \frac{1}{2} \operatorname{var}(P_{t_1} - P_{t_2}) \quad , \tag{6}$$

where it is assumed that the variance of the difference $P_{t_1} - P_{t_2}$ for any two points t_1 and t_2 only depends on their horizontal distance $||t_1 - t_2||$, see e.g. Montero *et al.* (2015) .

[†]The Voronoi cell of s_i consists of those locations in W that are closer to s_i than to any other grid point. In our particular example of application the Voronoi cells of all grid points that are not located at the boundary of the observation window are squares with sides of 20 km length.

An estimate $\hat{\gamma}$ of the semivariogram can be computed based on $p_{s_1}, \ldots, p_{s_n}$ using an iterative algorithm. Furthermore, for each r' from a sequence $\{r_1, \ldots, r_k\}$ of possible precipitation cell radii, we determine the corresponding intensities $a'_1, \ldots, a'_n$ as described in Sec. 3.2.1 with fixed radius r', compute point probabilities according to (4) and determine, using the same iterative algorithm, an estimate $\hat{\gamma}^{(r')}$ based on obtained point probabilities. The radius r of the precipitation cells for the current weather finally results as best fit

$$r = \underset{r' \in \{r_1, \ldots, r_k\}}{\operatorname{argmin}} \left\{ \int_{c_1}^{c_2} \left(\hat{\gamma}^{(r')}(h) - \hat{\gamma}(h) \right)^2 dh \right\} \quad , \qquad (7)$$

where the integrals are evaluated numerically and c_1 and c_2 are some suitable integration limits. As a compromise between covering a sufficiently large variety of possible radii and allowing computations to be done in a reasonable time we choose $k = 9$ and $\{r_1, \ldots, r_k\} = \{7.5\,\text{km}, 10\,\text{km}, \ldots, 27.5\,\text{km}\}$.

3.3. *Prediction of area probabilities*

Having computed the intensity parameters $a_1, \ldots, a_n$ and the precipitation cell radius r, the estimation of area probabilities is straight forward. Similar as for point probabilities we assume that there is precipitation within an area B if and only if there is an intersection of B with at least one precipitation cell. The union set M of precipitation cells with radius r intersects the area B, if at least one point of the random set $\{X_i, i = 1, \ldots, Z\}$ of cell centres falls into the enlarged area $B^r = \{t \in W : \min_{b \in B} ||b - t|| \leq r\}$. The generalisations of (3) and (4) read

$$n(B^r) = \sum_{j=1}^{n} a_j \, |B^r \cap V(s_j)| \qquad (8)$$

for the expected number of cell centres within B^r and

$$\pi(B) = 1 - e^{-\sum_{j=1}^{n} a_j \, |B^r \cap V(s_j)|} \qquad (9)$$

for the area precipitation probability $\pi(B)$.

As the numerical computation of the intersections $B^r \cap V(s_j)$ according to (9) is expensive, area probabilities can also be estimated using Monte Carlo simulation. A large number of realisations of the random union set M in (2) is generated using highly efficient simulation algorithms, see, e.g. Møller and Waagepetersen (2004), and the area probability $\pi(B)$ is estimated as the relative frequency of intersections with area B. About 1,000 realisations of M are sufficient to obtain precise precipitation probabilities for arbitrary areas that can be defined ad hoc.

4. Validation of area probabilities

A validation of the modeled area probabilities is carried out with the following approaches. Independent radar data is used as an area covering observation system for verification. Various scores of the area probabilities are computed for areas with different sizes and shapes, see Sec. 4.1. The impact of the estimated cell radius r is addressed in Sec. 4.2 as it plays an important role in terms of the spatial correlation of precipitation. Furthermore a comparison with uncalibrated area probabilities of the COSMO-DE-EPS is provided in Sec. 4.3.

4.1. *Verification with radar data*

4.1.1. *Description of radar data*

The area probabilities of precipitation are verified with radar–derived precipitation analyses from the German operational radar network of DWD, see Winterrath *et al.* (2012). The DWD radar network consists of 16 sites covering Germany and provides precipitation scans every five minutes. Radar reflectivities are transformed into precipitation rates using empirical reflectivity–precipitation rate (Z-R) relationships. For every hour precipitation amounts are derived and adjusted using about 1300 rain gauges at conventional meteorological measurement sites in order to provide adjusted quantitative precipitation analyses. An additional clutter filter for hydrological applications removes spurious pixel–scale precipitation events, see Winterrath and Rosenow (2007).

The minimum analysed precipitation amount per hour is 0.1 mm, the threshold value for the MOS–derived point probabilities has been set accordingly (see Sec. 2.3) in order to allow for consistent verification. The relative frequencies of analysed radar precipitation events are in good agreement with the forecasts of both point and area probabilities as confirmed in the following.

4.1.2. *Verification results*

The stochastic model of precipitation cells proposed in Sec. 3 allows for an estimation of precipitation probabilities for arbitrary areas. In order to obtain verification areas with various sizes, shapes and orientations, a homogeneous Poisson point process has been generated in the observation window and the verification areas are chosen as the cells of the resulting Voronoi tessellation. A mean number of 1400 points is chosen that was found to provide a reasonable selection of smaller and larger verification areas. The verification areas are displayed in Fig. 1 along with forecast biases, Brier skill scores, and observed frequencies of precipitation. The Brier skill score is computed using as reference the relative frequency over time for each grid point or Voronoi cell, respectively. Verification is only performed where coverage of radar data is sufficient. For the scores only one–, two– and three–hourly forecasts are recorded in order to avoid multiple use of observations by overlapping forecasts in time. The quality of the area probabilities of course depends on the underlying point forecasts. In Tab. 1 mean verification scores for point and area probabilities are listed in order to assess the impact of the stochastic model. Additionally the empirical correlation coefficient between area probability and observed precipitation is included. No additional bias is introduced when propagating the precipitation probabilities from points into areas, which is an important issue in terms of calibrated probabilistic forecasts. Since the point forecasts are statistically calibrated (see Sec. 2.2) retaining calibration for the area probabilities is desired. Furthermore, there is no conditional bias given the size of the area, as Fig. 1 (left) indicates.

score	point prob.	area prob.
bias	-1.17 (+/-0.012)	-1.00 (+/-0.019)
BSS	0.236 (+/-0.059)	0.316 (+/-0.064)
corr	0.492 (+/-0.056)	0.58 (+/-0.046)

Table 1. Mean verification scores for point and area probabilities: Bias in percentage points, Brier skill score (BSS), and empirical correlation coefficient (corr). The numbers in brackets denote the standard deviations of the verifications scores.

The other scores, Brier skill score and correlation coefficient are even improved for the area probabilities, which reveals that the area probabilities correspond very well to the radar observations. The spatial distribution of Brier skill scores given in Fig. 1 (centre) shows, in combination with the frequency of precipitation (right), that this score is highest for areas with lots of precipitation in the south of Germany. These high Brier skill scores originate from the

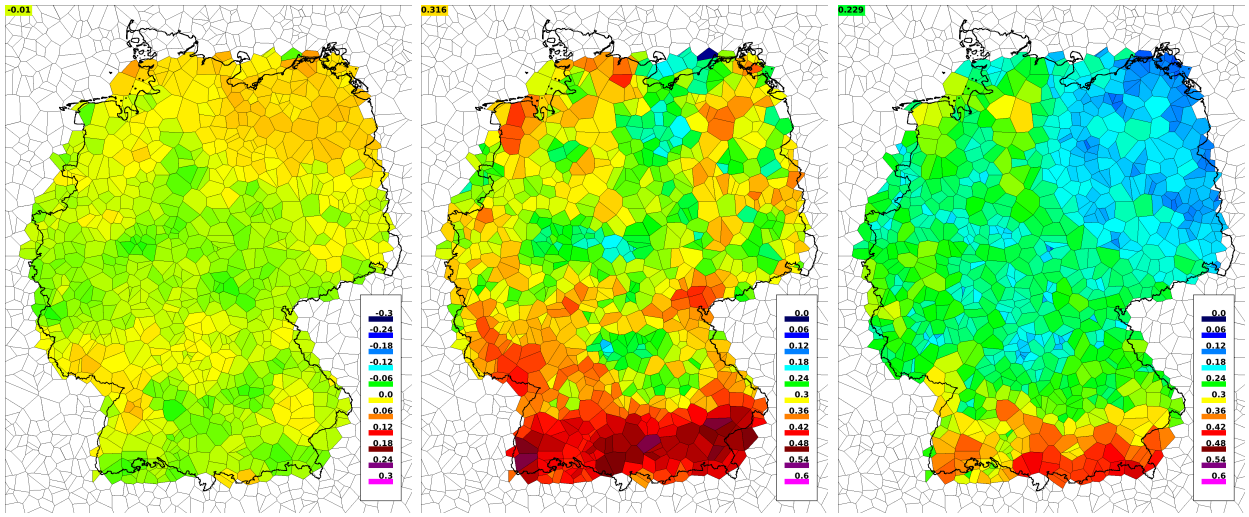

Figure 1. Scores of area probabilities for a selection of forecast areas: bias (left), Brier skill score (centre), frequency of precipitation (right)

point forecasts, but are also retained for the area probabilities. The empirical correlation coefficients have highest values for the areas with most precipitation events, too.

Figure 2 provides reliability diagrams of point and area probabilities that show the relative frequency of precipitation events according to radar observations for bins of forecasted precipitation probabilities. Whereas the point probabilities are well calibrated, being close to the ideal line of identity in general, the area probabilities show slight underforecasting for low and stronger overforecasting for high probabilities. This indicates that the area probabilities have a slightly lower statistical resolution and are little more over–confident than the underlying point forecasts. Bin–wise confidence intervals of the probabilities are very small due to the large number of observations and not shown therefore.

This issue may be related to the sizes of the cell radii and is further addressed in Sec. 4.2 .

4.2. *Impact of precipitation cell radii*

The sizes of precipitation cells determine the spatial correlation structure of the modeled precipitation patterns. Their impact on area probabilities is as follows: smaller cells cause higher area probabilities in general. This meets the meteorological expectation that small scale convection shows higher spatial variability than large scale events. Higher variability leads to an increased probability that there is precipitation anywhere in an area. The stochastic model estimates higher intensities for smaller cell radii and generates more precipitation cells in order to fit the point forecasts. That correspondingly results in increased probabilities that a precipitation cell intersects an area in question. When using the optimal radius between 7.5 km and 27.5 km according to the method prescribed in Sec. 3.2.2, the bias of area precipitation probabilities is negligible with -1.0 percentage points. The biases for the optimal radius and for fixed radii of 7.5 km and 27.5 km are listed in Tab. 2 . In accordance to theoretical expectations smaller radii cause larger probabilities and thus positive biases and vice versa. Due to the large number of data the results are considered significant, compare the standard deviations in Tab. 1 . This shows that the estimation of cell radii has an significant impact and that the selected radii are well chosen according to the resulting area probabilities.

Figure 3 (left) displays the histogram of the determined radii of one–, two– and three–hourly forecasts. Most frequently radii of 10 km are selected, which can be considered physically reasonable for events of convective precipitation that occurred frequently in

radius	7.5 km	7.5–27.5 km	27.5 km
bias	5.4	-1.0	-7.6

Table 2. Bias of area precipitation probabilities in percentage points with constant radii of 7.5 km, best fit between 7.5 km and 27.5 km, and constant radii of 27.5 km

the considered period. The distribution of larger radii is more or less uniform but much more radii of 27.5 km appear. The radii have been restricted to a maximum value of 27.5 km a priori, however, since larger radii would be rarely chosen and the computation time would increase unnecessarily.

The point forecasts are updated every three hours, so that for a forecast length of 10 hours up to four forecasts for the same valid time exist (e.g. a 10–hour forecast issued 02 UTC is valid for 12 UTC and is updated three hours later by the 7–hour forecast issued at 05 UTC, etc.). Figure 3 (right) presents the distribution of changes of radii between older and newer forecasts for the same valid time. Most often the radius is unchanged, which shows that the selection method of the radius is stable and does not change erratically with slightly changed point forecasts. In operational applications computation costs are saved if the radii can be reused for later updates of the forecasts.

A lag-1 autocorrelation coefficient of 0.42 was found that reflects persistency in time of the evolving precipitation patterns and the resulting cell radii from one hour to the next. The coefficient is remarkably large when considering that the radii of the precipitation cells are assumed to be constant across the forecast area and that a local change in weather regime at some place has impact on the globally selected radii. It is certainly also possible that the globally fixed radius of precipitation cells is the reason for the missing statistical resolution as indicated in the reliability diagram of the area precipitation probabilities in Fig. 2 (right). The point probabilities (Fig. 2, left) show a very weak underforecasting for probabilities between about 0.1 to 0.2 and a stronger overforecasting for probabilities between about 0.5 and 0.8 . The area probabilities amplify this distinctive behaviour which results in underforecasting for probabilities between about 0.1 and 0.4 and overforecasting for probabilities of 0.6 and more. Generally the area probabilities are higher than the point probabilities, which can also be seen in the histograms of Fig. 2 (although the total number of forecasts is slightly different). There is a large number of point forecasts close to 0 and the numbers decrease with the height of the point probabilities. For

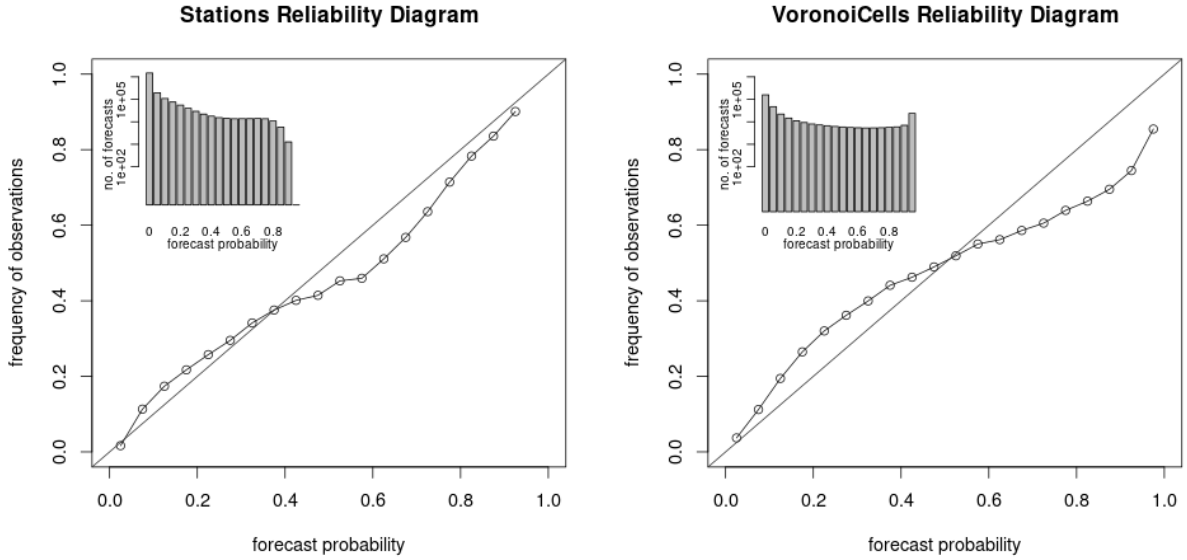

Figure 2. Reliability diagrams of point (left) and area probabilities (right)

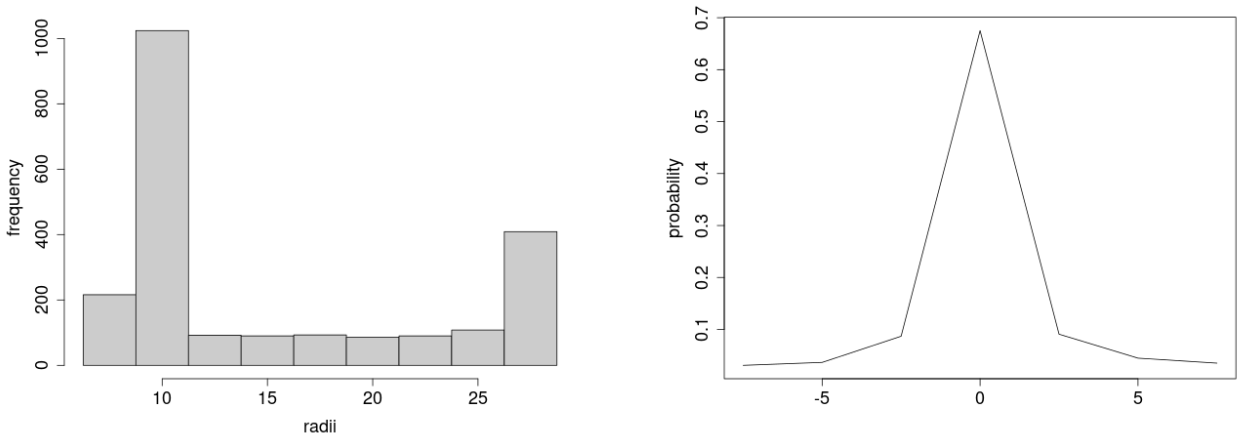

Figure 3. Histogram of precipitation cell radii in km for one–, two– and three–hourly forecasts (left). Distribution of changes of radii in km with forecast updates (right)

the area probabilities there is a decrease up to around 0.7 only, thereafter the numbers of forecasts with higher area probabilities increase, showing a particularly large number of forecasts with probabilities close to 1 . It was found that neither reliability nor histogram of area probabilities significantly depend on the sizes of areas, which indicates that our stochastic model is suitable for arbitrary areas. We expect that simply in- or decreasing the radii of precipitation cells would just lead to a forecast bias and cannot adjust for both the underforecasting (for lower probabilities) and overforecasting (for higher probabilities) simultaneously. To obtain a better resolution more variation in the radii or location-dependent radii to better account for regional weather conditions could be suitable, however. But, in general, statistical resolution is limited by the underlying point probabilities.

4.3. Comparison with raw upscaled ensemble probabilities

In order to conclude model validation, area precipitation probabilities obtained from the stochastic model described in Sec. 3 are compared to the upscaled raw ensemble estimates introduced in Sec. 2.1 . For comparison purposes, area probabilities are derived based on our stochastic model for the same grid of 28 km resolution as the upscaled ensemble probabilities. The point probabilities are derived not before two hours after the start of the COSMO-DE-EPS in order to ensure its computation has finished. One–hourly point forecasts, for example, are therefore based on three–hourly forecasts of the ensemble. Consequently, area probabilities from our stochastic model for lead times of one, two and three hours are matched with the corresponding three–, four– and five–hourly forecasts of the ensemble. Figure 4 displays biases and Brier skill scores of area probabilities in 28 km resolution computed by our stochastic model. The results are qualitatively similar to those for the random decomposition into Voronoi cells presented in Fig.1 with small biases in general and high Brier skill scores in the south of Germany where lots of rain occurred during the verification period. The corresponding ensemble estimates are considered in Fig. 5 and show small negative biases and lower Brier skill scores in general. Especially in the south the high Brier skill scores of our stochastic model cannot be reached.

Table 3 summarises the scores of Figs. 4 and 5 and additionally includes the mean empirical correlation coefficient between predicted precipitation probabilities and observed precipitation as well as the mean standard deviation of forecasts. The scores of the area probabilities based on our stochastic model are comparable with those of the verification areas considered in Tab. 1 . There

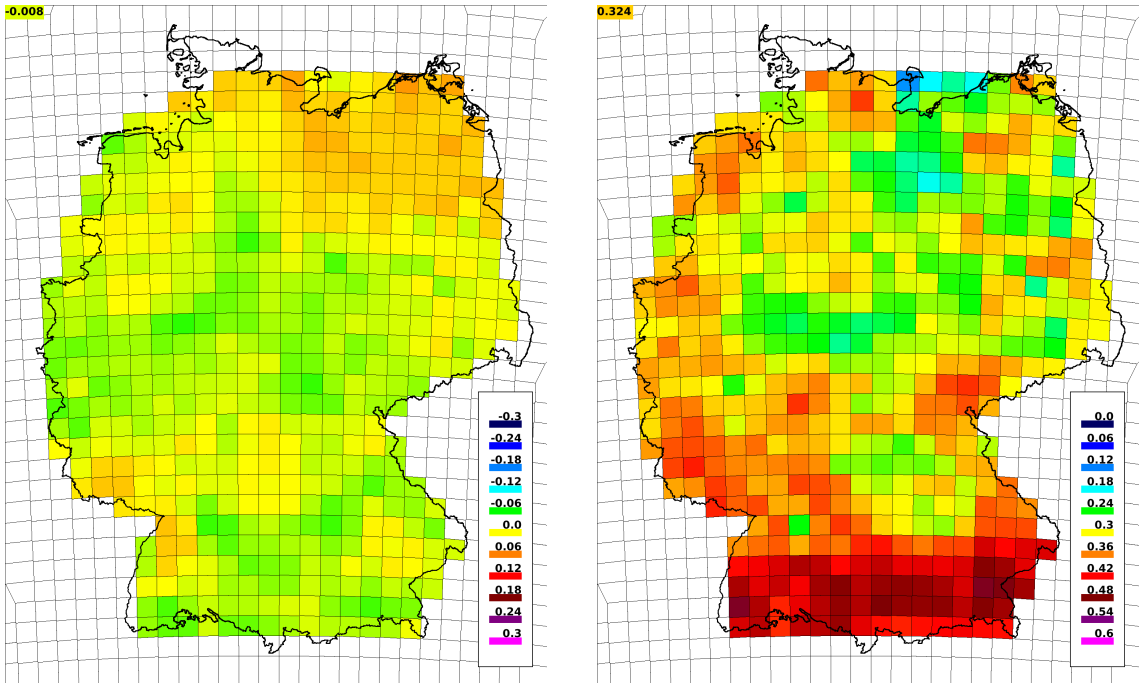

Figure 4. Bias (left) and Brier skill score (right) of area probabilities derived from the proposed stochastic model for the quadratic cells of a regular 28 km grid

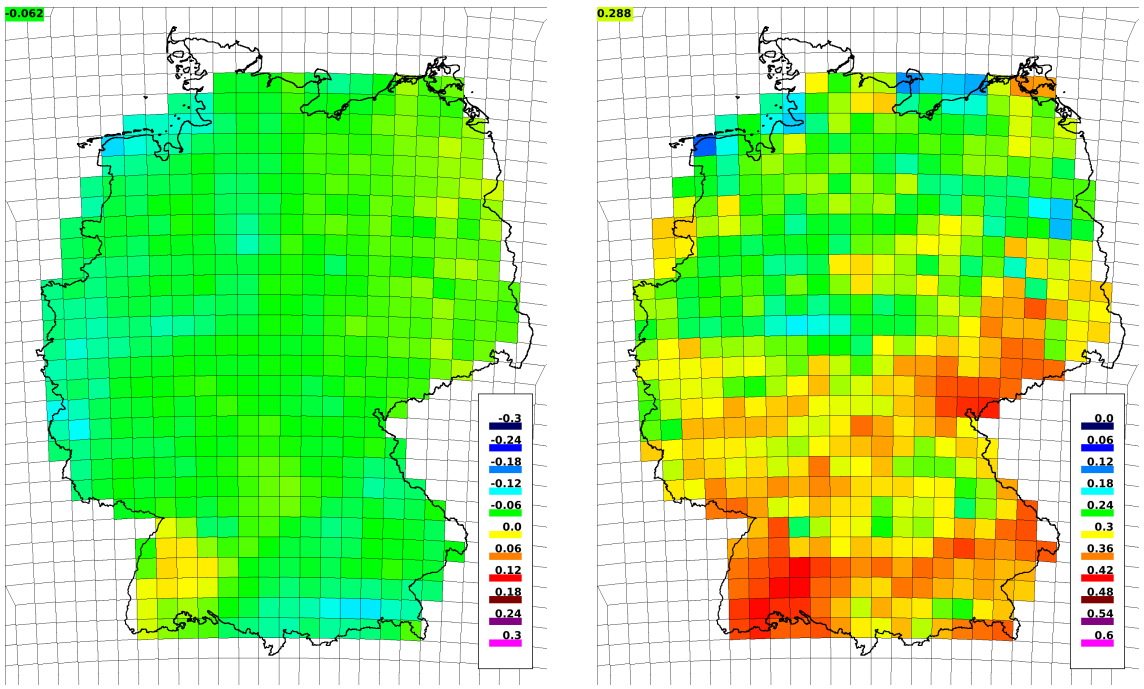

Figure 5. Bias (left) and Brier skill score (right) for upscaled raw ensemble estimates for the quadratic cells of a regular 28 km grid (corresponding to Fig. 4)

score	point prob	area prob.	ensemble prob.
bias	-1.17	-0.8	-6.2
BSS	0.236	0.324	0.288
corr	0.492	0.591	0.582
stdev	0.288	0.315	0.319

Table 3. Mean verification scores for point and area probabilities: Bias in percentage points, Brier skill score (BSS), correlation coefficient between predicted precipitation and observed precipitation (corr) and standard deviation of forecasts (stdev) in percentage points

is a mean bias of -6.2 percentage points for the upscaled probabilities from the ensemble and a significantly smaller mean Brier skill score, indicating that the proposed stochastic model outperforms the raw ensemble. The mean correlation coefficients are comparable, however. Also the mean standard deviations of point and area forecasts are almost equal, which shows that the improved mean Brier skill score of the stochastic model is not obtained by reduced statistical sharpness.

5. Conclusion and Outlook

In the present paper a recently developed approach to the computation of area probabilities based on models and methods from stochastic geometry as introduced in Kriesche *et al.* (2015) is motivated, discussed and evaluated from a meteorological point of view. As a result, the area probabilities derived by

means of this stochastic modeling approach are qualified to be used operationally for the automated generation of specific user products on arbitrary areas. Calibration of point probabilities for precipitation is well preserved for area probabilities, which is considered essential in high quality probabilistic forecasting.

The comparison of the stochastically modeled area probabilities with upscaled relative frequencies of the raw COSMO-DE-EPS reveals essential advantages of the stochastic model in terms of bias and Brier skill score. The upscaled relative frequencies based on raw ensemble members correspond well with radar data given they are not calibrated, though, showing a good quality of the COSMO-DE-EPS for probabilistic precipitation (on the upscaled 28 km scale). The high Brier skill scores in Southern Germany that result from the stochastic model could not be reached, however. It is not clear, anyway, how to calibrate them with synoptic ombrometer data. A stringent calibration would require a relationship between area precipitation and point measurements, where methods of stochastic geometry would probably be appropriate again.

So far, the optimal precipitation cell radius is globally estimated based on the available forecasts of point probabilities. Its size has a significant impact on the estimated area probabilities, not only theoretically, but as is also clearly seen in our forecast verification. However, the territory of Germany is large and often various weather regimes appear simultaneously, which requires a compromise for the estimation of the optimal global radius. Locally estimated radii could lead to more differentiating and sharper area probabilities. Additional data seems to be required for this, e.g. model fields of the COSMO-DE-EPS.

The proposed methods of stochastic geometry are suitable for further applications in operational weather forecasting where, in particular, forecast of strong precipitation events are of great interest for warning management at DWD. As a first step towards this need, Kriesche *et al.* (2017b) generalised the stochastic model considered in the present paper for precipitation amounts and for the probabilities that given thresholds of precipitation rates are exceeded.

The stochastic approach of modeling area probabilities is considered applicable for other meteorological variables as well, but calibration and verification depends on whether appropriate observations are available. For example, area probabilities for strong screen–level wind gusts would be of great interest. Proper evaluation seems problematic, however, as area–based observations or observations with high spatial and temporal resolution are not available. For wind gusts verification is considered mandatory, since orography and other land surface properties are highly relevant. Note that an approach for the modeling of thunderstorm cells has been proposed in Kriesche *et al.* (2017a), which is based on lightning data as an area covering observation system.

Finally, as a prerequisite of operational use, the stochastic model considered in the present paper has been technically implemented as a test product at DWD that derives predefined area probabilities for several resolutions based on point forecasts of precipitation that are generated within AutoWARN. As the estimation of the optimal global radius is the main computational effort, the stochastic model has been optimised so that the global radii of previous forecasts are used as initial values for the optimisation for subsequent forecasts.

Acknowledgements

Thanks to Tanja Winterrath and Elmar Weigl, for providing information on clutter correction and on gauge adjusted radar data in general. For preprocessing and providing the radar data we thank Tamas Hirsch.

References

Baldauf M, Seifert A, Förstner J, Majewski D, Raschendorfer M, Reinhardt T. 2011. Operational convective–scale numerical weather prediction with the COSMO model: description and sensitivities. *Mon. Weather Rev.* **139**(12): 3887–3905.

Bowler NE, Pierce CE, Seed AW. 2006. STEPS: A probabilistic precipitation forecasting scheme which merges an extrapolation nowcast with downscaled NWP. *Q. J. R. Meteorol. Soc.* **132**(620): 2127–2155.

Chiu SN, Stoyan D, Kendall WS, Mecke J. 2013. *Stochastic Geometry and its Applications*. J. Wiley & Sons: Chichester, 3rd edn.

Epstein SE. 1966. Point and area precipitation probabilities. *Mon. Weather Rev.* **94**(10): 595–598.

Gebhardt C, Theis SE, Paulat M, Bouallègue ZB. 2011. Uncertainties in COSMO-DE precipitation forecasts introduced by model perturbations and variation of lateral boundaries. *Atmos. Res.* **100**: 168–177.

Hamill TM, Engle E, Myrick D, Peroutka M, Finan C, Scheuerer M. 2017. The U.S. national blend of models for statistical postprocessing of probability of precipitation and deterministic precipitation amount. *Mon. Weather Rev.* **145**(9): 3441–3463.

Hess R, Glashoff J, Reichert BK. 2015. The Ensemble-MOS of Deutscher Wetterdienst. In: *EMS Annual Meeting Abstracts*, 12. Sofia.

Knüpffer K. 1996. Methodical and predictability aspects of MOS systems. In: *Proceedings of the 13th Conference on Probability and Statistics in the Atmospheric Sciences*. San Francisco, pp. 190–197.

Kriesche B, Hess R, Reichert BK, Schmidt V. 2015. A probabilistic approach to the prediction of area weather events, applied to precipitation. *Spat. Stat.* **12**: 15–30.

Kriesche B, Hess R, Schmidt V. 2017a. A point process approach for spatial stochastic modeling of thunderstorm cells. *Probab. Math. Stat.* (in print).

Kriesche B, Koubek A, Pawlas Z, Beneš V, Hess R, Schmidt V. 2017b. On the computation of area probabilities based on a spatial stochastic model for precipitation cells and precipitation amounts. *Stoch. Environ. Res. Risk Assess.* (in print). DOI:10.1007/s00477-016-1321-8.

Krzysztofowicz R. 1998. Point–to–area rescaling of probabilistic quantitative precipitation forecasts. *J. Appl. Meteorol.* **38**: 786–796.

Møller J, Waagepetersen RP. 2004. *Statistical Inference and Simulation for Spatial Point Processes*. Chapman & Hall/CRC: Boca Raton.

Montero J–M, Fernández-Avilés G, Mateu J. 2015. *Spatial and Spatio–Temporal Geostatistical Modeling and Kriging*. J. Wiley & Sons: Chichester.

Onof CJ, Chandler RE, Kakou A, Northrop PJ, Wheater HS, Isham VS. 2000. Rainfall modelling using Poisson-cluster processes: A review of developments. *Stoch. Environ. Res. Risk Assess.* **14**(6): 384–411.

Reichert BK. 2010. AutoWARN – automatic support for issuing weather warnings. *promet* **35**(1/2): 98–103.

Reichert BK. 2017. Forecasting and nowcasting severe weather using the operational warning decision support system AutoWARN at DWD. In: *9th Europ. Conf. on Severe Storms ECSS*. Pula, Croatia.

Reichert BK, Glashoff J, Hess R, Hirsch T, James P, Lenhart C, Paller J, Primo C, Raatz W, Schleinzer T, Schröder G. 2015. The decision support system AutoWARN for the weather warning service at DWD. In: *EMS Annual Meeting Abstracts*, 12. Sofia.

Schefzik R, Thorarinsdottir TL, Gneiting T. 2013. Uncertainty quantification in complex simulation models using ensemble copula coupling. *Statist. Sci.* **28**(4): 616–640.

Wheater HS, Chandler RE, Onof CJ, Isham VS, Bellone E, Yang C, Lekkas D, Lourmas G, Segond M-L. 2005. Spatial-temporal rainfall modelling for flood risk estimation. *Stoch. Environ. Res. Risk Assess.* **19**(6): 403–416.

Wheater HS, Isham VS, Cox DR, Chandler RE, Kakou A, Northrop PJ, Oh L, Onof CJ, Rodriguez-Iturbe I. 2000. Spatial-temporal rainfall fields: Modelling and statistical aspects. *Hydrol. Earth Syst. Sci.* **4**: 581–601.

Wilks DS. 2011. *Statistical Methods in the Atmospheric Sciences*. Academic Press: San Diego, 3rd edn.

Winterrath T, Rosenow W. 2007. A new module for the tracking of radar–derived precipitation with model–derived winds. *Adv. Geosci.* **10**: 77–83.

Winterrath T, Rosenow W, Weigl E. 2012. On the DWD quantitative precipitation analysis and nowcasting system for real–time application in German flood risk management. In: *Proceedings of an International Symposium on Weather Radar and Hydrology*. Exeter, pp. 323–329.

